AIAA JOURNAL
Vol. 43, No. 1, January 2005

Dual-Band Infrared Imagery of an Atlas 5 Launch Vehicle in Flight

Arnold Goldberg*
U.S. Army Research Laboratory, Adelphi, Maryland 20783

Imagery acquired with a quantum-well infrared photodetector dual-band infrared focal plane array of the inaugural launch of the Atlas 5 launch vehicle is presented. The focal plane array was developed under the U.S. Army Research Laboratory's Advanced Sensors Federated Laboratory program and used a read-out integrated circuit produced under the Air Force Research Laboratory's Advanced Multi-Quantum Well Technology program. The detectors are able to sense light in both the 3–5- and 8–12-μm atmospheric transmission windows such that the resulting single-band images are pixel registered and simultaneous. The focal plane array was installed in a camera system that used a closed-cycle cooler to operate at 60 K. The camera was placed at the prime focus of an all-reflective telescope on a computer-controlled tracking mount at the Innovative Sensor Technology Evaluation Facility at the Kennedy Space Center. The launch was observed from a distance of 15 km from the pad. The dual-band camera system was calibrated using standard blackbody sources. The launch vehicle was observed from about 30 s after launch until approximately 4 min after launch. This corresponded to ranges between 15 km and more than 300 km and altitudes from just over 1 km to more than 100 km. Several interesting differences in the structure of the plume were observed. In addition, the hardbody of the rocket was seen in the 8–12-μm imagery but was undetectable in the 3–5-μm imagery. The imagery was unsaturated in both bands allowing us to obtain good measurements of the radiance of the plume in both the principal infrared bands.

Introduction

ONE of the principal strategies contemplated for defending against an intercontinental-ballistic-missile (ICBM) attack is to intercept the missiles soon after they are launched while their booster engines are still firing. This so-called boost-phase intercept (BPI) is advantageous because the rocket plumes have a large infrared (IR) signature that can be detected and tracked from a far distance and the rockets can be destroyed with a relatively small impact from a kill vehicle.

The Earth's atmosphere is relatively transparent in two "windows" of the IR spectrum, one between wavelengths of 3 and 5 μm (the so-called medium-wavelength infrared or MWIR) and a second between wavelengths of 8 and 14 μm (the so-called long-wavelength infrared or LWIR). It is a law of physics that all objects at temperatures above absolute zero emit electromagnetic radiation (light). The temperature of the object and its emissivity determine the spectrum of the emitted light and its intensity. Hot objects like rocket plumes emit most of their energy at wavelengths in the visible and MWIR, whereas objects near room temperature emit most of their light in the LWIR. The hot gases that make up the plumes have emission spectra that do not closely match that of a blackbody, especially in the MWIR band where CO_2 and H_2O have strong emission bands. On the other hand, the plume emission in the LWIR is expected to be close to that of a blackbody. Blackbody radiation is, by its nature, an equilibrium process, whereas the hot gases that make up a rocket plume are likely to not be in a state of equilibrium. The nonequilibrium distribution of molecular and atomic energy states is likely to cause enhanced IR emission over and above that which would be expected from a blackbody at the temperature of the plume.

Over the past few years, the field of infrared imaging has undergone rapid progress. Large-format focal plane arrays (FPAs) have been produced that can capture high-quality images of a scene at video frame rates. In addition, much effort has been put into producing multicolor FPAs that are sensitive to more than one region of the IR spectrum. The Army Research Laboratory (ARL), in collaboration with several industry and academic partners under the Advanced Sensors Collaborative Technology Alliance (ASCTA), is developing the sensor technologies necessary for the Army's Future Combat System (FCS). This sensor system is envisioned as a single unit combining both passive and active sensor components with advanced-signal-processing and aided-target-recognition tools. Such a sensor would enhance situational awareness on the battlefield in all ambient conditions by locating and classifying threats with increased effectiveness over existing systems. An integral part of the FCS sensor system is a dual-band infrared imager operating in the MWIR and LWIR bands. This imager would be advantageous over single-color IR cameras (either LWIR or MWIR) because it can operate in a wider range of ambient conditions and be more effective in defeating IR countermeasures such as smoke, camouflage, and flares. The ASCTA (and its predecessor the Advanced Sensors Federated Laboratory) program has supported research aimed at producing large-format, staring, dual-band FPAs. Dual-band FPAs such as those developed in the ASCTA program can easily be applied to other defense and commercial applications.

The MWIR and LWIR signatures of rocket vehicles and their plumes in boost phase are of great importance to the Missile Defense Agency (MDA). It is well known that the rocket plume presents a large MWIR signal that can be detected and tracked at large distances (hundreds of kilometers). However, for the BPI mission just described, it is necessary to image not only the bright rocket plume but, simultaneously, the hardbody of the missile as well. The missile hardbody has its strongest emission in the LWIR part of the spectrum. The LWIR signature of the plume is large relative to that of the hardbody, but it is small relative to the plume's MWIR signature. Therefore, for the boost-phase-intercept mission it will be advantageous for the sensor on the kill vehicle to have a dual-band MWIR/LWIR FPA such as those developed under the ASCTA program. This paper describes the acquisition and analysis of dual-band IR signature data from the Atlas 5 launch vehicle using a dual-band quantum-well infrared photodetector (QWIP) FPA produced by BAE Systems (formerly Sanders, a Lockheed Martin Company), in collaboration with researchers at ARL under the Federated Laboratory program. This rocket is similar in many ways to strategic ICBM threat vehicles.

Received 11 February 2004; revision received 6 July 2004; accepted for publication 4 August 2004.

*Physicist, EO/IR Technology Branch.

Experimental Setup

Dual-Band FPA

The dual-band FPA used in this study has been described previously.[1] The FPA was made using the QWIP[2] detector structure. The device structure is shown schematically in Fig. 1. The pixels were square with a 40-μm pitch in both the x and y directions. The space between pixels was less than 2 μm, leading to a fill factor of greater than 84% in the MWIR detectors (bottom layer) and greater than 77% for the LWIR detectors (top layer). The measured normalized spectral response for each of the bands is shown in Fig. 2. The effective spectral width, defined as the integral of the normalized spectral response function over all wavelengths, or

$$W = \int_0^\infty R(\lambda)\, \mathrm{d}\lambda \ \mu\mathrm{m} \tag{1}$$

where $R(\lambda)$ is the normalized spectral response function, was found to be 0.584 μm for the MWIR and 1.042 μm in the LWIR.

The read-out integrated circuit (ROIC) was designed by Lockheed Martin Missiles and Fire Control Systems under the Air Force's Advanced Multiple Quantum Well Technology program. The simultaneously integrating and windowing ROIC was fabricated by using a 0.5-μm complementary metal-oxide semiconductor process. It is designed to consume less than 50 mW of power with a 5-V supply, it uses a switched-capacitor, frame snapshot architecture capable of frame rates up to 180 Hz, and it can provide variable bias for each color. The capacitance of the integration capacitor can be selected with a serial word command. In low-gain mode, the capacitance of the charge well is 1 pF, and in high-gain mode the capacitance is 0.1 pF [well capacity 2.5×10^7 and 2.5×10^6 electrons, respectively, for drain-to-drain voltage (VDD) = 5 V]. This ROIC has also been used for dual-band LWIR/LWIR and MWIR/MWIR imaging FPAs.[3]

The device architecture is such that the bias on the MWIR and LWIR stacks can be controlled independently. This is an important feature because the responsivity of QWIPs is proportional to bias. Therefore, the responses of the MWIR and LWIR portions of the FPA can be balanced through a combination of adjustments to the bias levels and the internal gain (charge well size) of the ROIC.

The FPA was installed in a camera Dewar with a cold stop focal ratio of $f/2.5$. The FPA was cooled using a split-linear closed-cycle cooler to an operating temperature of 60 K. The FPA was run using commercially available CamIRa™ hardware and software. Real-time 14-bit digital image data were collected on a disk array at a frame rate of 51.5 frames/s (data rate of 13.17 MB/s) using commercially available hardware and software.

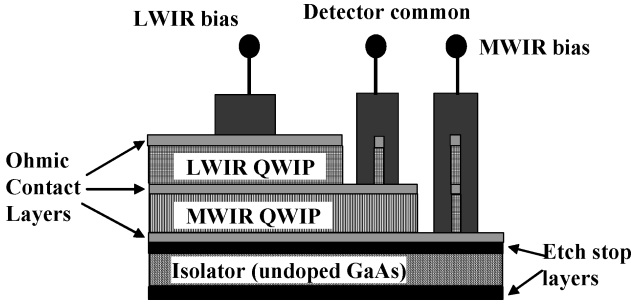

Fig. 1 Schematic representation of the dual-band QWIP detector structure.

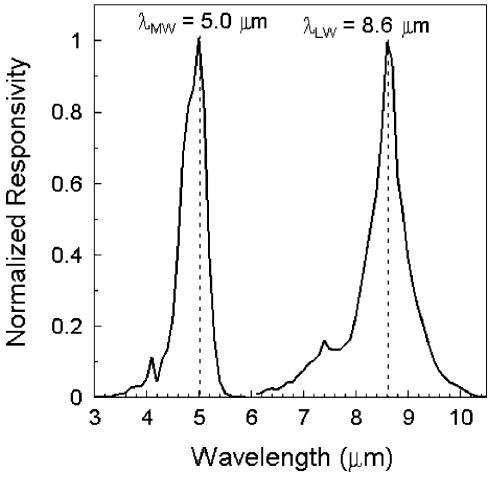

Fig. 2 Normalized response spectra for the MWIR and LWIR sections of the dual-band QWIP FPA.

Launch Vehicle

Recently, the U.S. Air Force has developed a series of launch vehicles known collectively as the evolved expendable launch vehicle (EELV). These include the Atlas 5 produced by Lockheed Martin and the Delta 4 made by Boeing. The inaugural launch of the Atlas 5 was on 21 August 2002; the inaugural launch of the Delta 4 was 20 November 2002.

The Atlas 5 uses a Russian-built (RD AMROSS) RD-180 engine with two nozzles. The Atlas 5 can be produced in several different configurations depending on the mission. The configuration used on the inaugural flight—the launch of the Hot Bird 6 communications satellite—did not use any solid rocket boosters and used the 15-m Centaur upper stage; this vehicle configuration is designated as "401." Figure 3 shows the Atlas 5 in the 401 configuration. The first stage fires for approximately 4 min. During the latter stages of the first stage burn, the engine is throttled back to keep the vehicle's acceleration less than $5g$. After shutdown, the vehicle coasts for approximately 10 s until the first stage is jettisoned and the second stage (Centaur) is ignited. It was anticipated that if the weather were clear the vehicle could be observed throughout the duration of the first stage burn and the staging events.

Observation Platform

The launches were observed from the Innovative Science and Technology Evaluation Facility (ISTEF) of MDA located at the Kennedy Space Center, Cape Canaveral, Florida. The observation site was approximately 15 km southwest of the launch pad. The dual-band infrared camera was placed at the prime focus of an all-reflective telescope. The telescope's objective mirror was 12.5 in. (31.75 cm) in diameter, and the focal length was 150 in. (381 cm) giving a focal ratio of $f/12$. Because the FPA pixel size was 40 μm, the instantaneous field of view for each pixel was 10.5 μrad, and the total field of view was 2.69 mrad (0.154 deg). In testing the configuration of the telescope, imagery of commercial air traffic at cruising altitude was collected. Figure 4 shows an image of a Boeing 737 aircraft (rear view) at an estimated range of 34 km. The MWIR image shows only the engines, whereas the LWIR image shows the airplane's fuselage and wings.

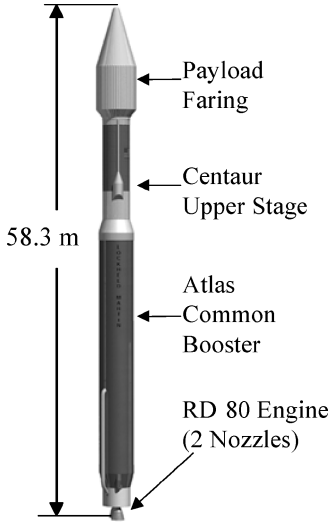

Fig. 3 Atlas 5 EELV in the 401 configuration. Data available online at http://www.ils-launch.com.

Radiometric Calibration Sensor

To obtain radiometrically calibrated imagery, the camera system's response to standard blackbody sources was measured in two configurations. First, in the bench calibration configuration, the FPA was flood illuminated by an extended-area blackbody source at a number of temperatures with no imaging optics and defined by the $f/2.5$ cold stop. Next, in the field calibration configuration the FPA/optics system was used to image the extended-area blackbody (at a number of temperatures) at a range of approximately 200 m from the telescope. These radiometric calibrations were performed after nonuniformity correction (NUC) was done on the raw data from the FPA. For the NUC a blank (cloudless) patch of sky at an elevation angle of 45 deg was used as the cold source and a heated black plate (temperature approximately 80°C) as the hot source. Two-point NUCs were performed for four different FPA operational setups using integration times ranging from 0.5 to 4 ms. During the launch observation, only the shortest (0.5 ms, designated as low gain) and the longest (4 ms, designated as high gain) integration times were used.

Figure 5 shows the results of the field calibrations for the low and high gain configurations. The target radiance (determined by the blackbody temperature) is plotted against the output counts. From the observed linear relationships between radiance and output, the apparent target radiance in both the MWIR and LWIR bands can be calculated. The true radiance can then be calculated using the modeled atmospheric transmission in each band.

The mean responses of the MWIR and LWIR parts of the FPA in the bench and field configurations are shown in Fig. 6. The slopes

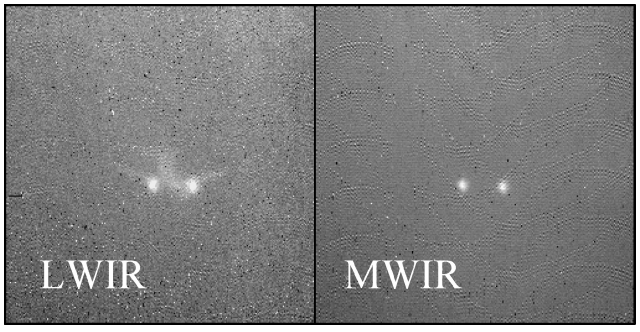

Fig. 4 Dual-band image of a Boeing 737 commercial aircraft at a range of approximately 30 km viewed with the ISTEF 12.5-in.-diam $f/12$ telescope.

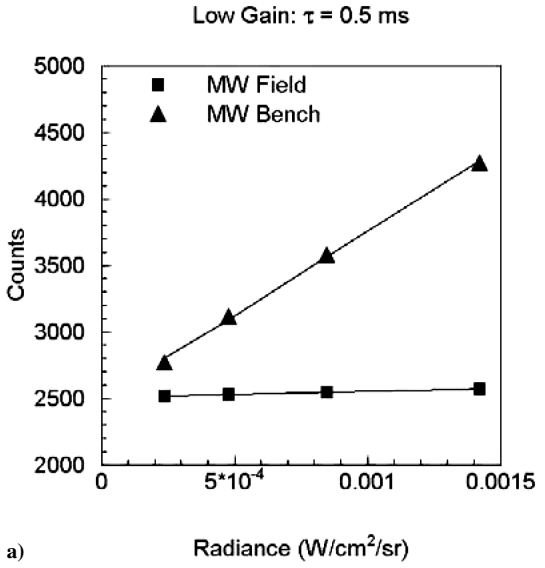

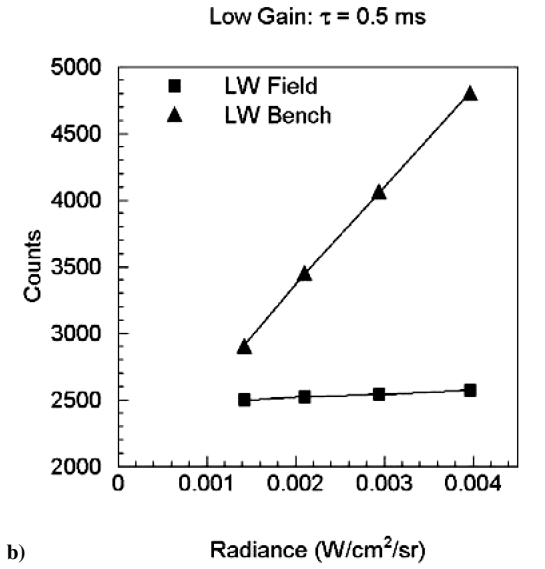

Fig. 6 Comparison of bench and field calibration curves for the a) MWIR and b) LWIR parts of the dual-band QWIP sensor.

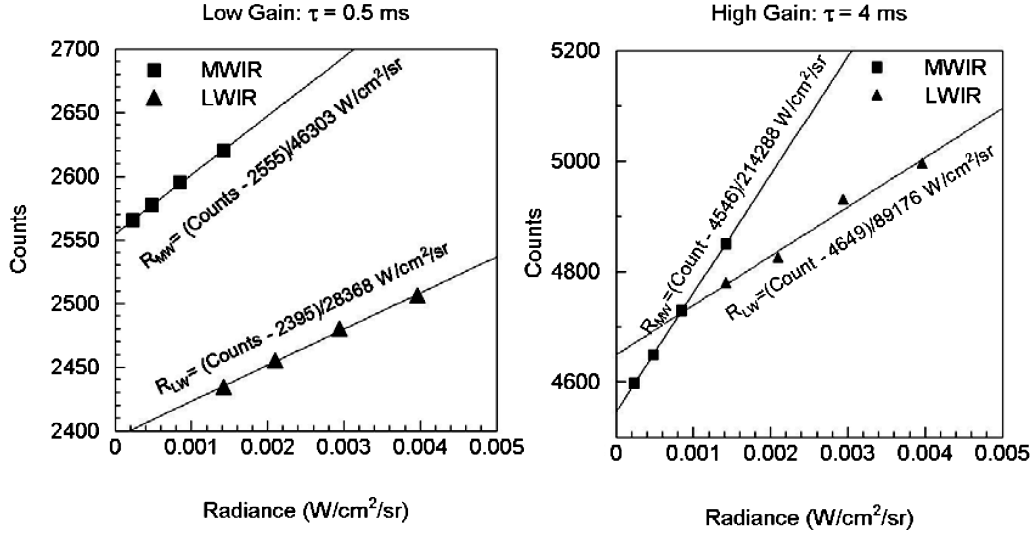

Fig. 5 Results of the field calibration of the dual-band QWIP sensor in the low gain and high gain configurations.

of the bench and field calibration curves in each band showed that there is a loss in sensitivity of a factor of 26.7 in both bands because of the imaging optics. Most of this loss can be accounted for by the change in optical throughput when going from the $f/2.5$ dewar aperture to the $f/12$ optical imaging system of the telescope (loss factor = 23.4). The majority of the remaining 13.7% in loss was caused by the obscuration of the primary mirror by the secondary flat mirror, which had a diameter of 10 in. All of these losses were independent of wavelength.

Atmospheric Transmission

To obtain accurate values for the radiance of the rocket plume, it is necessary to take into account atmospheric transmission losses. The U.S. Air Force Research Laboratory LOWTRAN model (version 7 from Ontar, Inc.) was used to calculate the atmospheric transmission based on a midlatitude summer atmospheric model over a spectral range from 800 cm^{-1} (12.5 μm) to 3000 cm^{-1} (3.33 μm) at a resolution of 5 cm^{-1}. If the normalized detector spectral response function is given as $R(\lambda)$ and the atmospheric transmission function is $t(\lambda)$, then the integrated atmospheric transmission is given by

$$T = \frac{\int t(\lambda)R(\lambda)\,d\lambda}{\int R(\lambda)\,d\lambda} \tag{2}$$

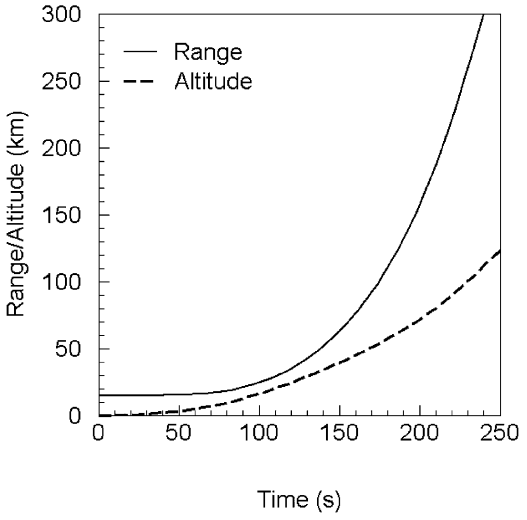

Fig. 7a Range and altitude vs time for the Atlas 5 launch of 21 August 2002 as observed from the ISTEF site.

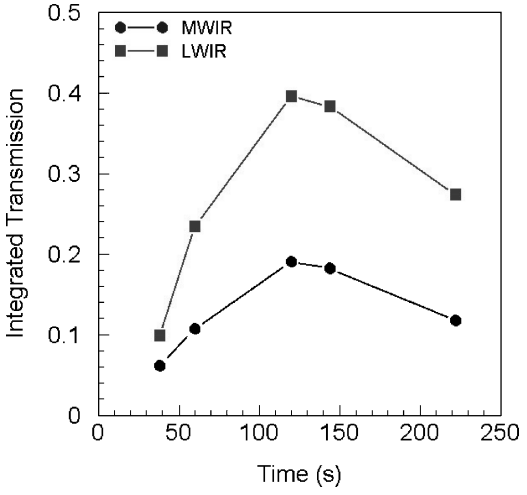

Fig. 7b Integrated atmospheric transmission for the MWIR and LWIR as functions of time after launch as calculated by the LOWTRAN model.

Equation (2) can be applied for each of the bands of the dual-band FPA separately by explicitly integrating the product of the atmospheric transmission function and the measured spectral response functions (over limits appropriate for each band).

Figure 7a shows the altitude and range of the Atlas 5 vehicle as a function of time as seen from the ISTEF site. The range to the launchpad was 14.93 km, and the rocket did not become visible from the ISTEF site until 34 s after launch because of obscuration from trees and buildings. At initial acquisition of the rocket was approximately 1 km high and 15 km downrange. The integrated atmospheric transmission was calculated for five points during the flight, 38, 60, 120, 144, and 220 s after launch. The transmission in each band is plotted as a function of time after launch in Fig. 7b. At first, the rocket is viewed over a long, mostly horizontal path, and the atmospheric absorption is relatively high. As the rocket climbs to higher elevations, it is viewed through progressively thinner slices of the atmosphere. As a result, the transmission increases up to the point of maximum elevation. Then, as the rocket heads downrange its elevation steadily decreases, and as a result it is observed through increasingly longer paths through the lower atmosphere. Thus the transmission decreases during the latter stages of the observation.

Results and Discussion

Plume Radiance

The inaugural launch of the Atlas 5 (mission number F5890) occurred at 22:05 GMT (6:05 pm EDT) on 21 August 2002. The vehicle was acquired with the dual-band IR camera at approximately 36 s after launch. Images of the MWIR and LWIR radiance are shown in Fig. 8; at this point in the flight, the rocket was at a range of 15.1 km and an altitude of 1.37 km. The radiance of the plume in the MWIR was considerably higher than that in the LWIR. In addition, the structure of the plume was noticeably different in the two bands. MWIR and LWIR images of the calibrated radiance of the plume at 60, 95, 120, 144, and 222 s after launch are shown in Figs. 9–13, respectively. The maximum radiance values in the MWIR and LWIR bands at each of these times are given in Table 1.

Early in the flight, the peak in-band MWIR and LWIR radiance of the plume are relatively constant at approximately 1.0 and 0.2 $W/cm^2/sr$, respectively. The radiance values correspond to blackbody temperatures of 2100 K in the MWIR and 1590 K in the LWIR. It is not surprising that these temperatures do not agree with each other because the plume is not expected to be a blackbody radiator. The presence of large amounts of hot CO_2 and H_2O would be expected to cause enhanced emission in the MWIR band. This extra emission would cause the blackbody temperature to appear to be higher than it really was in the MWIR. However, there are few molecular emission features in the part of the LWIR at which this detector was sensitive so that the blackbody temperature derived from the LWIR data is expected to be closer to the actual plume temperature. A smaller value of LWIR emissivity might also account for the lower blackbody temperature observed for this waveband.

Between $T + 95$ s and $T + 120$ s there is a dramatic decrease in the observed plume radiance in both bands. This might be caused by a number of reasons. During that portion of the flight, the vehicle was in transition from its vertical climb from the launchpad

Table 1 Range, altitude, and maximum MWIR and LWIR radiance at several times during the boost phase of the Atlas 5

T, s	Range, km	Altitude, km	Maximum MWIR radiance, $W/cm^2/sr$	Maximum LWIR radiance, $W/cm^2/sr$
38	15	1.37	1.1	0.17
60	15.76	4.67	1.0	0.179
95	21.5	14	0.96	0.21
120	35	24.4	0.44	0.107
144	55.75	36	0.3	0.08
222	228	91.5	0.066	0.0074

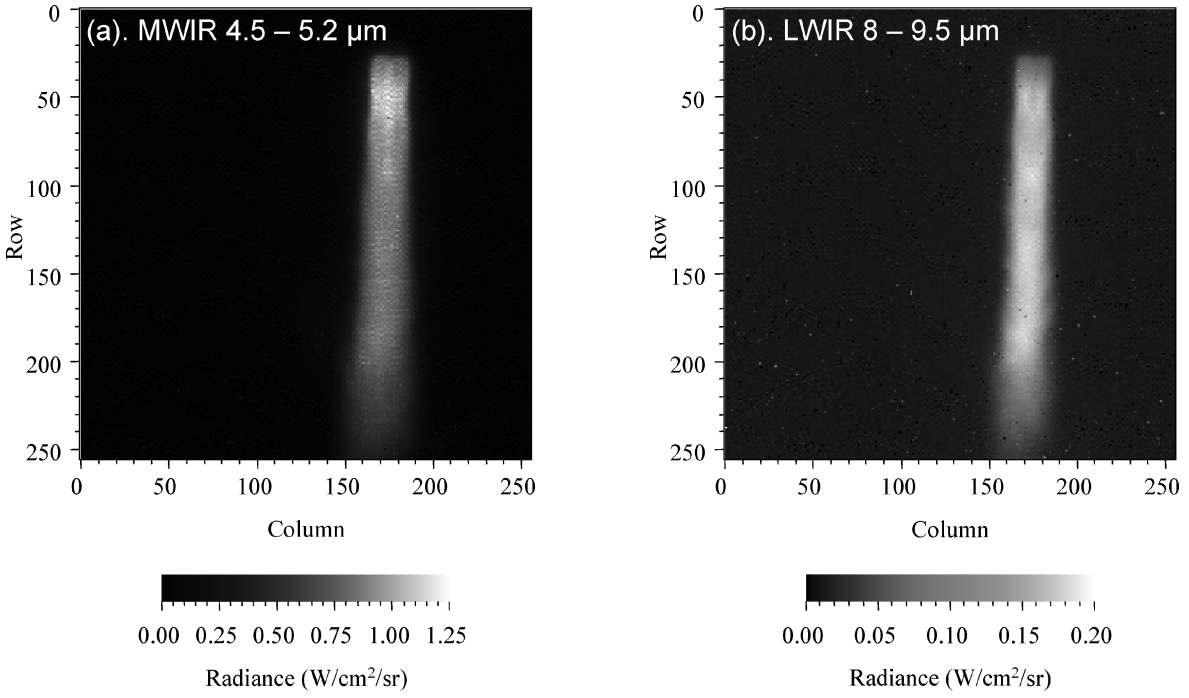

Fig. 8 Radiance images at $T + 38$ s.

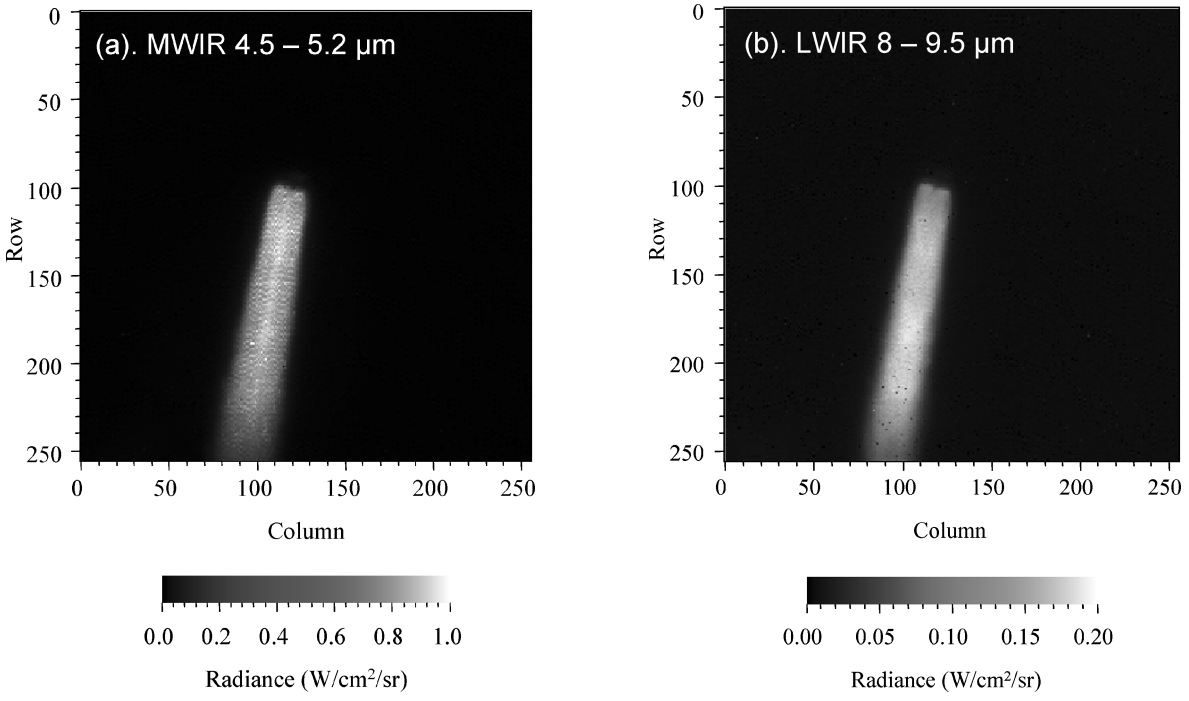

Fig. 9 Radiance images at $T + 60$ s.

to its course due east over the Atlantic. The viewing aspect of the plume changed significantly during the transition going from a mostly side aspect to an end-on aspect. In addition, the rocket was climbing into thinner parts of the atmosphere where there were fewer gas molecules with which the molecules of the plume could interact.

During the period from $T + 158$ s to $T + 215$ s, the vehicle was obscured by clouds, and no reliable signature data could be collected. From $T + 220$ s until the end of the collection, the sensor was operated in high-gain mode with an integration time of 4 ms. The plume radiance had become much smaller than in earlier parts of the flight. Only the central core of the plume close to the engine had an appreciable signature and the extended part of the plume was barely discernable in the MWIR image. From approximately $T + 224$ s to $T + 240$ s, the rocket's engine was throttled back to maintain a constant acceleration of $5g$ on the vehicle. Main engine cutoff was observed at $T + 241$ s. Very soon after that event, the vehicle was lost behind clouds, and it was not possible to observe the ignition of the second state.

Figure 14 shows the predicted MWIR and LWIR signatures of the plume for the Atlas 3 launch vehicle (whose first stage is nearly identical to that of the Atlas 5) and radiance calculated from

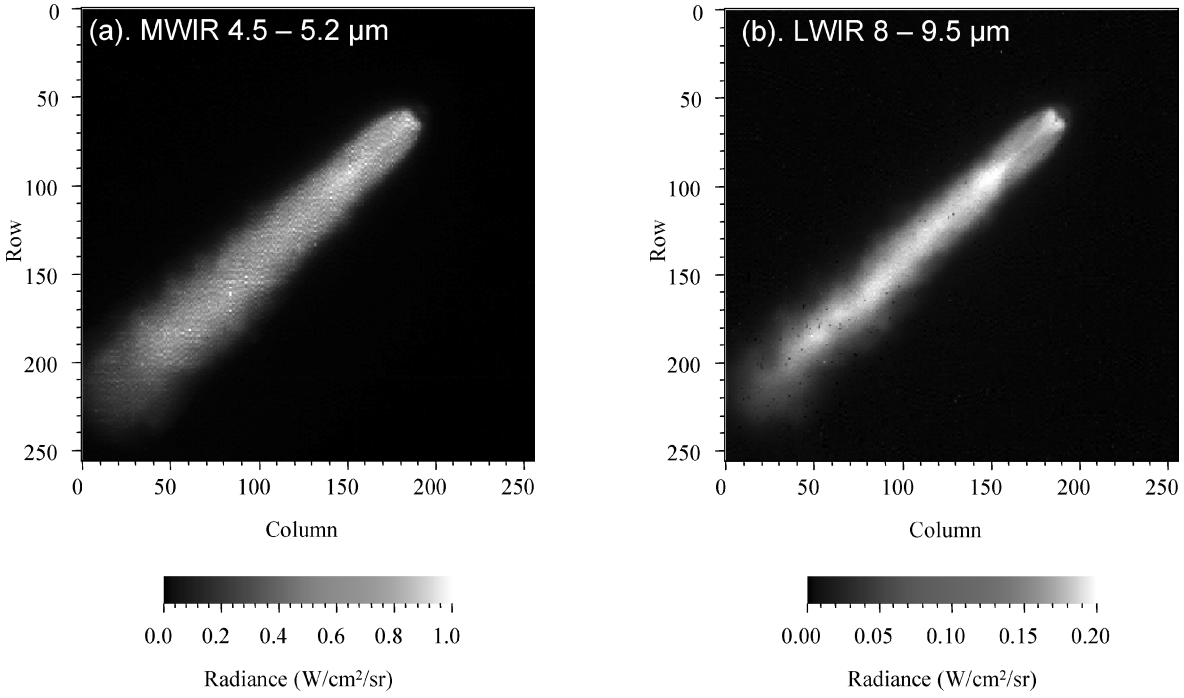

Fig. 10 Radiance images at $T + 95$ s.

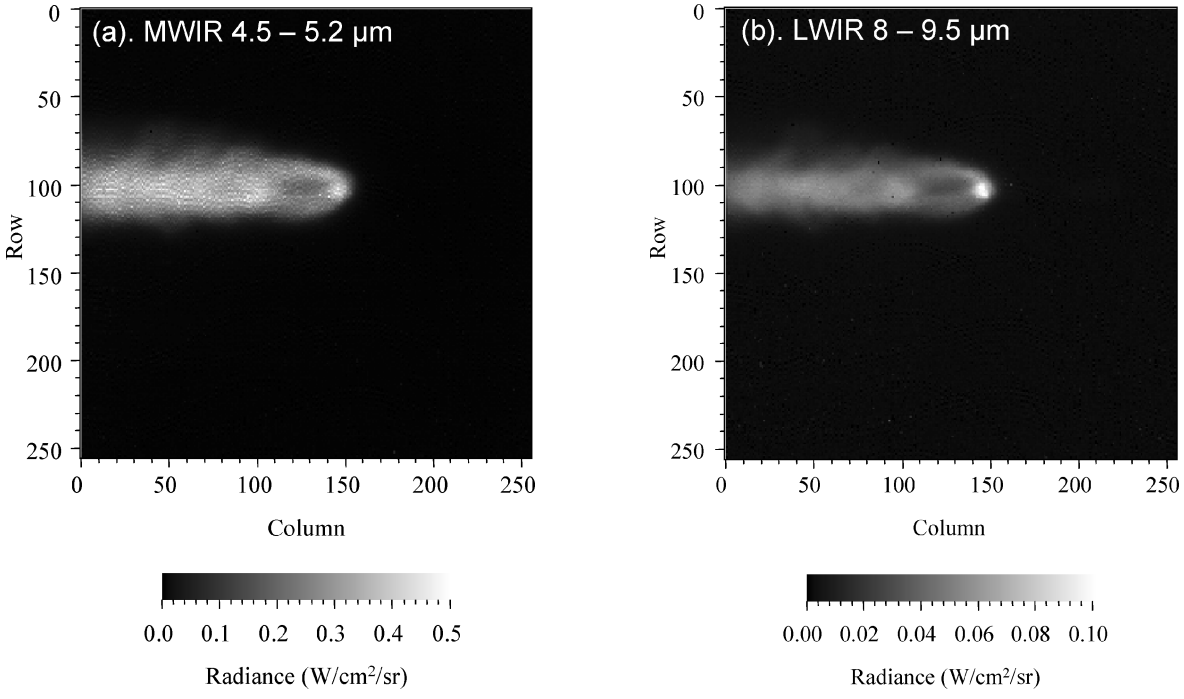

Fig. 11 Radiance images at $T + 120$ s.

measured data for the vehicle at an altitude of 15 km. The model, Flow Advanced Simulation Tool from Aero Optics, Inc.,[†] underestimated the maximum radiance of the plume by a factor of 2 in the MWIR and by a factor $\frac{5}{3}$ in the LWIR. In addition, the details of the structure seen in the real plume images were not predicted by the model. Most notably the bright line down the center of the plume (most visible in the MWIR) is not predicted at all in the model.

[†]Data available online at http://www.aero-optics.com/fast.html.

Missile Hardbody

One of the principal objectives of using the dual-band MWIR/LWIR FPA for this collection was to ascertain the detectability and visibility of the missile hardbody using the LWIR part of the FPA. Figure 15a shows the LWIR part of a dual-band image acquired 110 s after launch that has been enhanced to show the missile hardbody (and therefore, saturating the plume). The hardbody was not apparent in the MWIR image no matter how much gain was applied to the data. Because the signature of the hardbody is so low compared with that of the plume, both temporal and spatial filtering were applied to enhance its visibility.

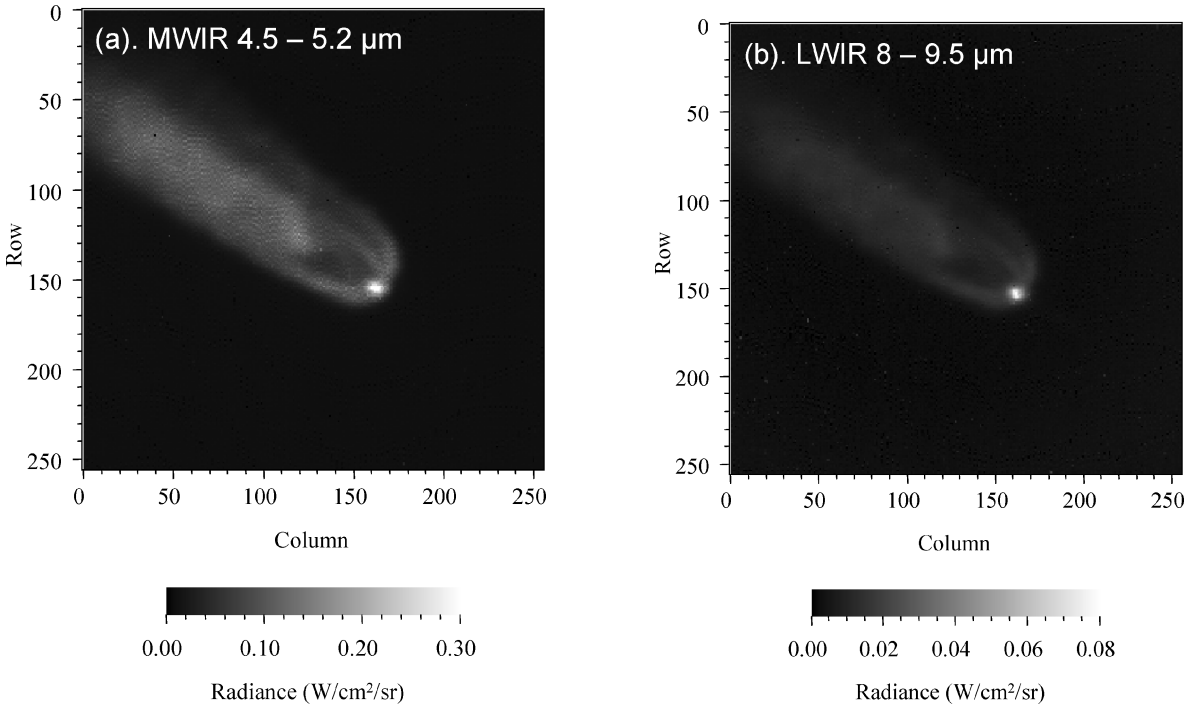

Fig. 12 Radiance images at $T + 144$ s.

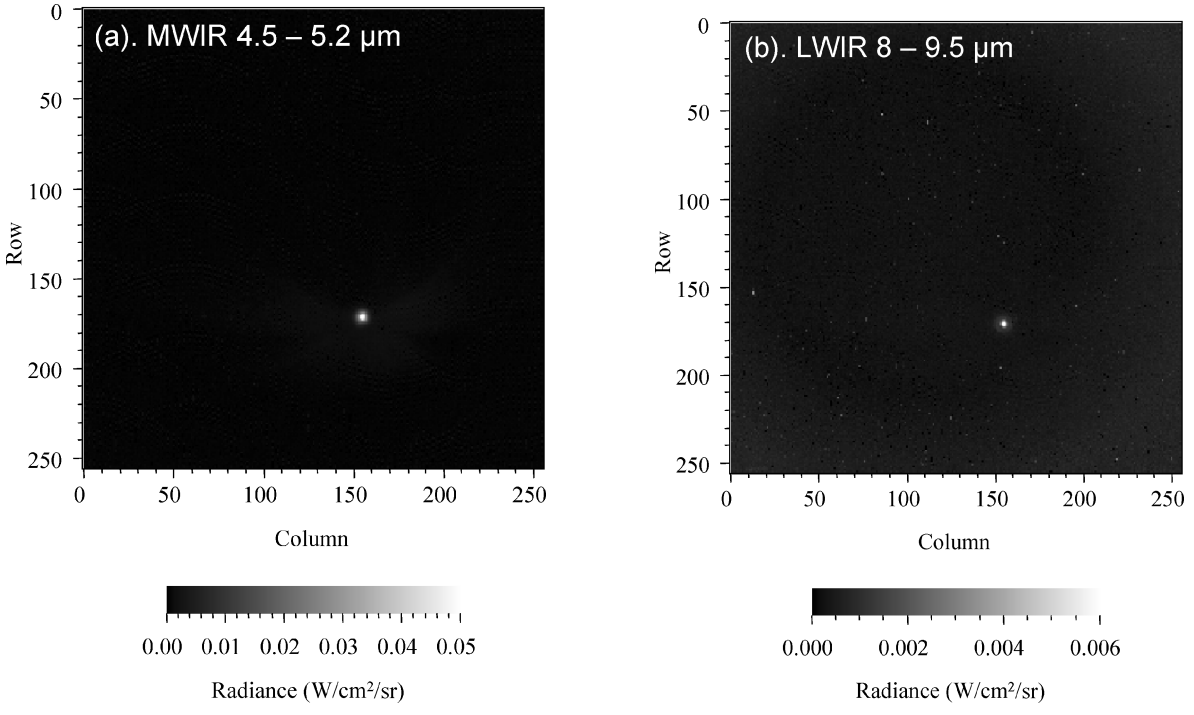

Fig. 13 Radiance images at $T + 222$ s.

Figure 15b shows the effect of averaging 10 consecutive frames (approximately 200 ms) to the image in Fig. 15a. Figure 15c shows the result of the application of a low-pass spatial filter with a cutoff frequency of half that of the maximum spatial frequency to the image in Fig. 15b. As a result of these processes, the Atlas 5 hardbody is clearly visible. The hardbody signature indicates that there is a region of cold surface temperatures from about the midpoint of the first stage to the beginning of the second stage. These cool surfaces are as a result of the presence of the cryogenic liquid-oxygen tank below this area of the first stage. It is also possible to resolve the shape of the payload faring at the nose of the vehicle.

Figure 16 shows the Atlas 5 hardbody in LWIR images acquired at $T + 120$ s, $T + 130$ s, and $T + 140$ s. These images were enhanced using the temporal and spatial filtering described above. As the vehicle flew downrange and turned toward the east, it became

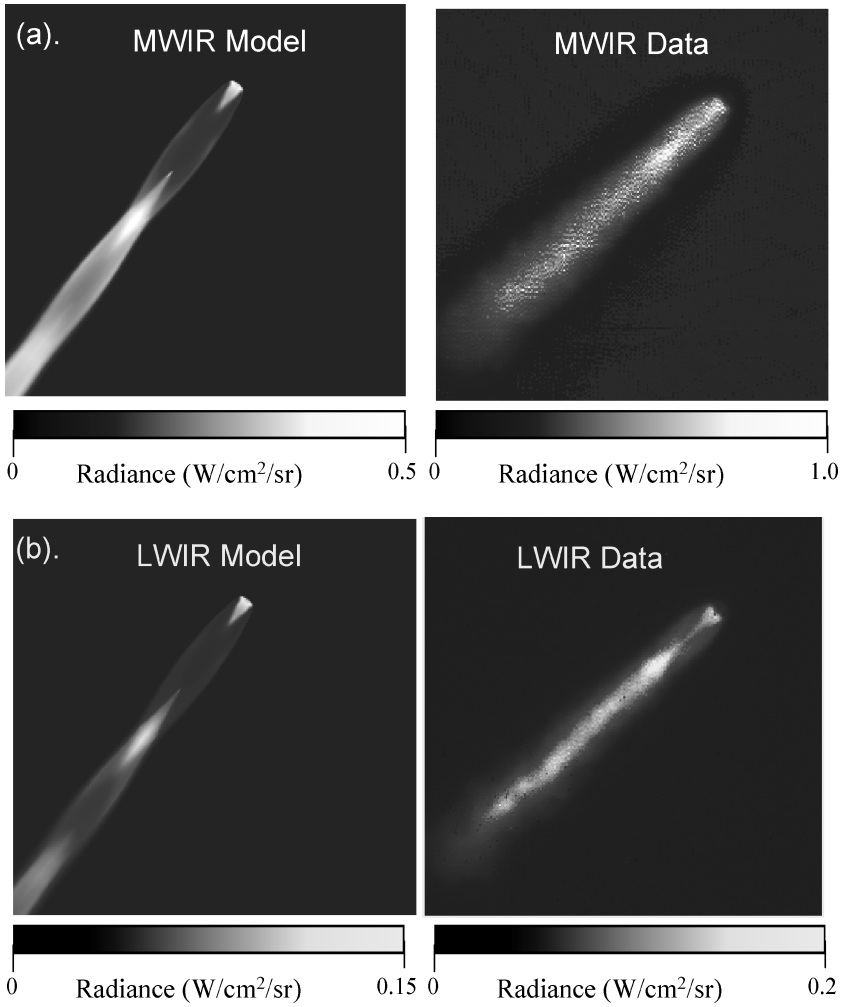

Fig. 14 Predicted radiance signatures compared with experimental data.

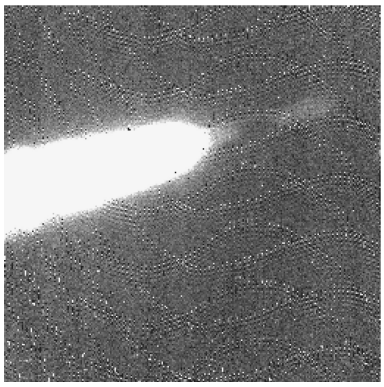

Fig. 15a Raw LWIR image at $T+110$ s showing Atlas 5 vehicle.

Fig. 15c Result of the application of a low-pass spatial filter to the image in Fig. 15b.

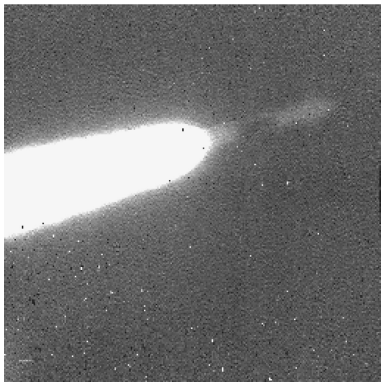

Fig. 15b Result of temporal averaging of 10 consecutive frames.

progressively less visible as a result of the change in aspect and obscuration by the plume.

Figure 17a shows the raw LWIR image acquired at $T+120$ s. The temporally and spatially filtered image is shown in Fig. 17b along with a magnified section of the image showing the Atlas 5 vehicle. Figure 17c shows a graph of the radiance along a profile of the hardbody (shown as a dashed line in Fig. 17b). The radiance of the hardbody is approximately 0.002 W/cm^2/sr, which corresponds to a temperature of 75°C (assuming an emissivity of one). The minimum hardbody radiance level is about 0.001 W/cm^2/sr, which is close to the background level. The corresponding upper limit on the temperature of the rocket body, in the vicinity of the cryogenic fuel tanks, is therefore about 30°C.

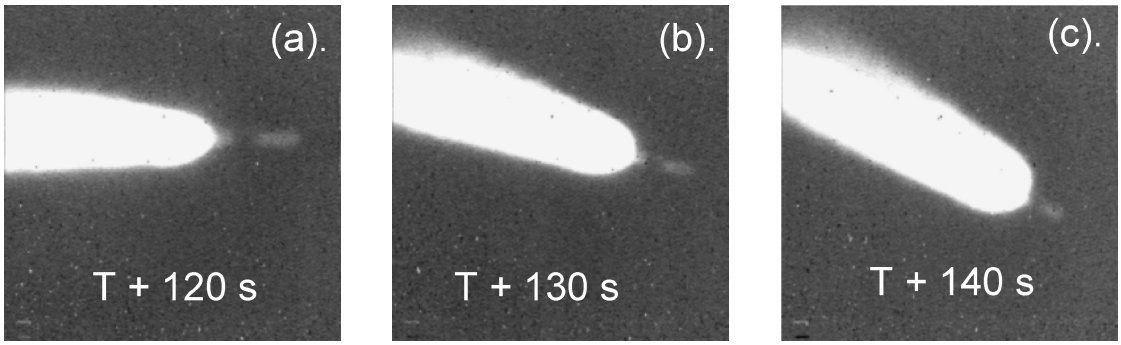

Fig. 16 Temporally and spatially filtered LWIR images showing the Atlas 5 hardbody.

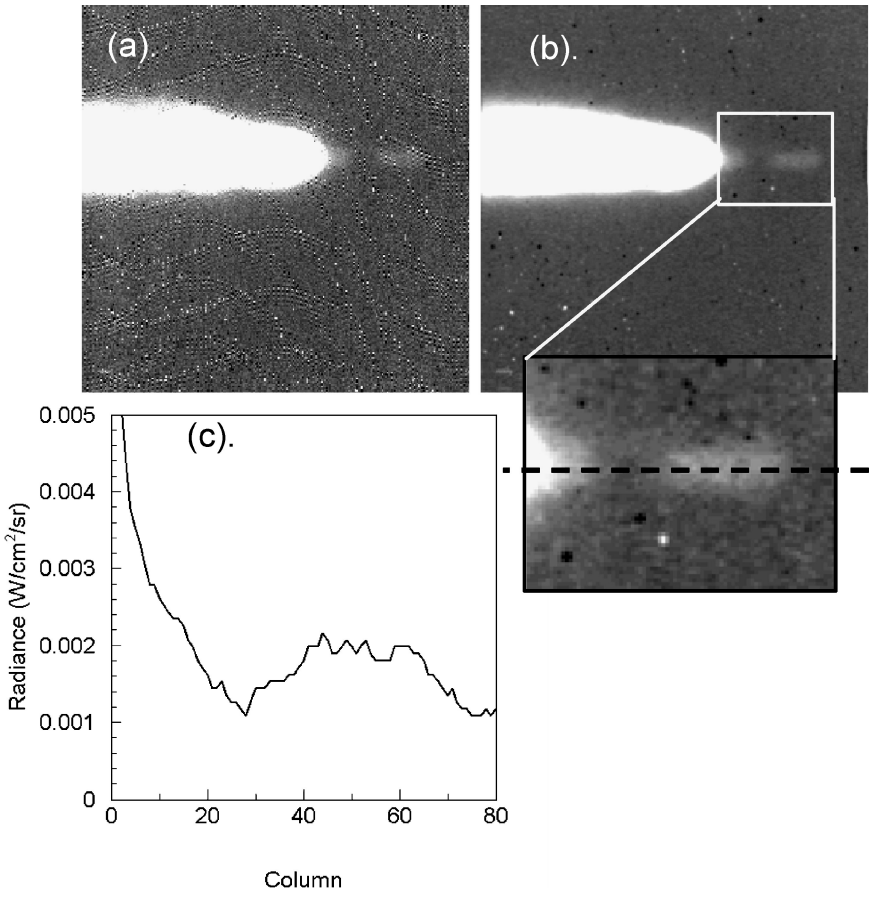

Fig. 17 Measurement of the radiance of the hardbody of the Atlas 5: a) raw LWIR image acquired at $T + 120$ s enhanced to show the Atlas 5 hardbody; b) temporal and spatial filtering applied to the image in panel a and a magnified section showing the Atlas 5; and c) line graph of the radiance of the Atlas 5 hardbody along the dashed line in panel b.

Summary

I have shown results of the application of a pixel-registered, simultaneously integrating dual-band infrared focal plane array operating in the medium-wavelength infrared (MWIR) and long-wavelength infrared (LWIR) spectral regions to the problem of imaging launch vehicles in the boost phase. The vehicle observed was the Lockheed Martin Atlas 5 during its initial launch in August of 2002. The Atlas 5 launch vehicle is a commercial analog to intercontinental ballistic missiles that pose a strategic threat to the United States. The entire boost phase until main engine cutoff at $T + 241$ s was observed.

The sensor system was radiometrically calibrated using standard blackbody sources. The collected imagery was unsaturated in both bands allowing us to calculate the plume radiance using both the sensor calibration and calculated values for atmospheric transmission during the flight. The maximum in-band radiance of the plume in the MWIR was approximately 1.0 W/cm^2/sr and that in the LWIR was approximately 0.2 W/cm^2/sr. These results were considerably higher than those predicted by a plume signature model in both bands. The difference between the model and the experimental data was approximately a factor of 2 in the MWIR and about $\frac{5}{3}$ in the LWIR. In addition, there were structures seen in the imagery of the plume that were not predicted in the model.

The hardbody of the Atlas 5 vehicle was apparent with gain enhancement in the LWIR imagery but not at all apparent in the MWIR imagery. The signal-to-noise ratio of the plume was considerably higher in the MWIR channel than that in the LWIR over the entire collection. Features such as the payload faring and the cool liquid-oxygen tank could be resolved in the LWIR images. At $T + 120$ s, the in-band LWIR radiance of the hardbody was approximately 0.002 W/cm^2/sr corresponding to a reasonable blackbody temperature of 75°C.

The dual-band focal plane array has been shown to be useful for the plume-to-hardbody handover function of a boost-phase-intercept missile defense mission. With additional signal processing,

it will be possible to view a fused MWIR/LWIR image that can give information from both bands in a real "color" image. Such images can give the seeker system the information on the plume and hardbody simultaneously that could significantly enhance the probability that the kill vehicle will intercept the target successfully.

Acknowledgments

I thank Mei-Mei Tidrow of Missile Defense Agency and Paul LeVan of U.S. Air Force Research Laboratory for support of these measurements. I also thank Michael Lovern of Navy SPAWAR for support of the Innovative Science and Technology Evaluation Facility (ISTEF) facility. Assistance at ISTEF for these measurements was provided by Alan Tietjen, Robert Patskowski, and Rolf Ahlgren. The read-out integrated circuit used for this work was designed and fabricated under the Advanced Multiple Quantum Well Technology program funded by the Air Force Research Laboratory, Contract F08630-96-C-0083, managed by David Hayden and John Winterberger.

References

[1]Goldberg, A., Kennerly, S., Little, J., Shafer, T., Mears, C. L., Winn, M., Taylor, M., and Uppal, P. N., "Comparison of HgCdTe and QWIP Dual-Band Focal Plane Arrays," *Optical Engineering*, Vol. 42, Jan. 2003, pp. 30–46.

[2]Choi, K. K., *The Physics of Quantum Well Infrared Photodetectors*, World Press, Singapore, 1997.

[3]Goldberg, A., Fischer, T., Kennerly, S., Wang, S., Sundaram, M., Uppal, P., and Winn, M., "Dual-Band QWIP MWIR/LWIR Focal Plane Array Test Results," *Proceedings of the Society of Photo-Optical Instrumentation Engineers*, Vol. 4028, edited by D. C. O'Shea, Society of Photo-Optical Instrumentation Engineers, Bellingham, WA, 2000, pp. 276–287.

R. Lucht
Associate Editor